Improved Laboratory Values of the H_2 Lyman and Werner Lines for Constraining Time Variation of the Proton-to-Electron Mass Ratio

E. J. Salumbides,[1] D. Bailly,[2,3] A. Khramov,[1] A. L. Wolf,[1] K. S. E. Eikema,[1] M. Vervloet,[3,4] and W. Ubachs[1]

[1]*Laser Centre, Vrije Universiteit, De Boelelaan 1081, 1081 HV Amsterdam, The Netherlands*
[2]*Laboratoire Photophysique Moléculaire, Université de Paris-Sud, Orsay, France*
[3]*Laboratorio de Espectroscopia e Laser, Instituto de Fisica, Universidade Federal Fluminense, Campus da Boa Viagem,*
Nitro, RJ 24210-340, Brazil
[4]*Synchrotron Soleil, L'orme des Merisiers, Saint-Aubin BP 48, 91192 Gif-sur-Yvette, France*
(Received 7 May 2008; published 26 November 2008)

Two distinct high-accuracy laboratory spectroscopic investigations of the H_2 molecule are reported. Anchor lines in the $EF^1\Sigma_g^+ - X^1\Sigma_g^+$ system are calibrated by two-photon deep-UV Doppler-free spectroscopy, while independent Fourier-transform spectroscopic measurements are performed that yield accurate spacings in the $B^1\Sigma_u^+ - EF^1\Sigma_g^+$ and $I^1\Pi_g - C^1\Pi_u$ systems. From combination differences accurate transition wavelengths for the $B - X$ Lyman and the $C - X$ Werner lines can be determined with accuracies better than $\sim 5 \times 10^{-9}$, representing a major improvement over existing values. This metrology provides a practically exact database to extract a possible variation of the proton-to-electron mass ratio based on H_2 lines in high-redshift objects. Moreover, it forms a rationale for equipping a future class of telescopes, carrying 30–40 m dishes, with novel spectrometers of higher resolving powers.

Fundamental physical constants may be subject to change on cosmological time scales. For the fine structure constant α, evidence for a temporal drift with a 5σ significance has been reported [1]. Recently, an indication of a possible decrease of the dimensionless proton-to-electron mass ratio $\mu = m_p/m_e$ was reported at $\Delta\mu/\mu = (2.45 \pm 0.59) \times 10^{-5}$ over a time interval of 12×10^9 years, based on a comparison of spectra of molecular hydrogen [2,3]. The latter findings require three crucial input ingredients. First, a theory is required that relates possible changes in μ to observable shifts in the spectrum of H_2. For this purpose sensitivity coefficients $K_i = d\ln\lambda_i/d\ln\mu$, which indicate how each line in the H_2 spectrum would drift as a result of a variation in the mass ratio μ, can be deduced either in a semiempirical fashion [3] or through quantum chemical *ab initio* calculations [4]. The second ingredient is the accurate determination of spectral line positions at high redshifts. Of the thousands of known quasar systems at redshifts $z > 2$, H_2 absorption features have only been observed in some 10 to 15 systems thus far. Of these, only Q0405-443 and Q0347-383 have high-quality and well-calibrated spectra containing many H_2 lines [5], which formed the basis of the finding on $\Delta\mu/\mu$ [2]. Recently, HE0027-184 was established as another system with many resolved H_2 lines [6], and hence a potential source in deriving further constraints on $\Delta\mu$. The final ingredient is a database comprising of high-precision laboratory measurements that represent present-day ($z = 0$) H_2 spectra. The limited amount of available astrophysical data accentuates the need for a set of laboratory data that would not contribute to the uncertainties in estimating a possible drift in μ.

The principle behind the novel determination of laboratory transition wavelengths in the $B^1\Sigma_u^+ - X^1\Sigma_g^+$ Lyman and the $C^1\Pi_u - X^1\Sigma_g^+$ Werner band systems is depicted in Fig. 1. Two entirely independent experiments are performed. First, the level energies of the lowest rotational states in $EF^1\Sigma_g^+$, $v = 0$ with respect to $X^1\Sigma_g^+$, $v = 0$ are
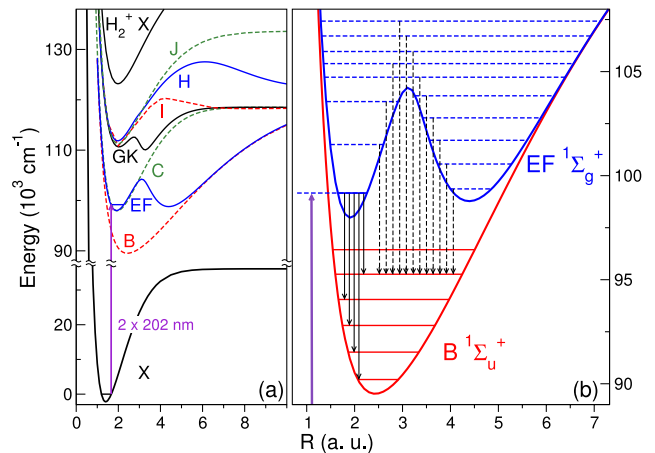

FIG. 1 (color online). Schematic of the combination differences exploited in this work. First, the two-photon frequency measurement (at $\sim 2 \times 202$ nm) on the $EF - X$ (0,0) system is used as the anchor to perform subsequent absolute calibrations, as indicated in (a). Two sets of transitions connecting the EF and B states are depicted in (b) to illustrate the technique. The transitions indicated by the solid arrows all originate from the EF $v = 0$ level and access different vibrational levels of B, leading to the calibration of the B levels. In a similar manner, the transitions indicated by the dashed arrows enable the calibration of the EF energy levels.

determined by deep-UV (DUV) two-photon laser excitation as depicted in Fig. 1(a). The EF $v = 0$, $J = 0$, 1 rotational levels then assume the role of anchors, on which all determinations of excited level energies will be based. A second experiment measures the energy differences between nearby lying levels in the $B^1\Sigma_u^+$ and $C^1\Pi_u$ states with respect to the EF anchor levels. As an illustration, two sets of transitions involving the $B - EF$ systems are highlighted in Fig. 1(b). The set represented by the solid arrows provides a measurement of the B vibrational energy levels relative to the anchor EF $v = 0$ level. In an analogous scheme, the transitions represented by the dashed arrows relate the upper EF levels to an arbitrary B vibrational level ($v = 4$) and hence can be used for the absolute calibration of the EF upper levels via the energy spacing between the B, $v = 4$ and the EF, $v = 0$ anchor.

The deep-UV spectroscopic determination of the $EF - X$ (0,0) rotational transitions have been described in detail by Hannemann *et al.* [7]. The experiment involves $2 + 1$ resonance-enhanced multiphoton ionization (REMPI) spectroscopy of H_2 at 202 nm; the deep-UV radiation is obtained from the frequency-quadrupling of the IR output from an injection-seeded Ti:sapphire oscillator-amplifier laser [8]. The Doppler *broadening* is minimized by utilizing the Doppler-free two-photon technique on a H_2 molecular beam (where the laser excitation beams are oriented perpendicular to the H_2 beam). Minimization of the residual Doppler *shift* is accomplished by exploiting a Sagnac interferometric alignment of the counter-propagating laser beams [9]. The high-resolution frequency calibration is achieved by referencing the cw-seeding radiation of the Ti:sapphire oscillator to a stabilized frequency comb referenced to a (GPS-disciplined) Rb-clock standard. Frequency offsets between the cw-seeding radiation and the IR pulse output of the oscillator are measured and corrected for in every laser pulse. In Fig. 2 typical two-photon spectra of the Q0 and Q5 lines are displayed. The accuracy in the frequency determination is estimated to be better than 2×10^{-9} [7].

The second experiment entails high-resolution Fourier-Transform (FT) spectroscopy, in a low pressure discharge of hydrogen, spanning a wide wavelength range from the midinfrared (5.5 μm) all the way to the violet (450 nm). The spectrum was obtained by a Bruker IFS 120 in four portions using appropriate filters and detectors (LN$_2$ cooled InSb photodiode, LN$_2$-cooled InGaAs photodiode, an avalanche silicon photodiode and a photomultiplier tube). As an example we show in Fig. 3 a spectrum at around 800 nm displaying the H_2 discharge emission lines from many band systems, including the $e^3\Sigma_u^+ - a^3\Sigma_g^+$ triplet systems that were reported recently in [10], where a detailed discussion about the FT experimental setup can be found.

The Fourier-transform spectra provide a database with a large information content. Because all relevant $B^1\Sigma_u^+$, v, J; $C^1\Pi_u$, v, J; and $EF^1\Sigma_g^+$, v, J rovibrational quantum levels
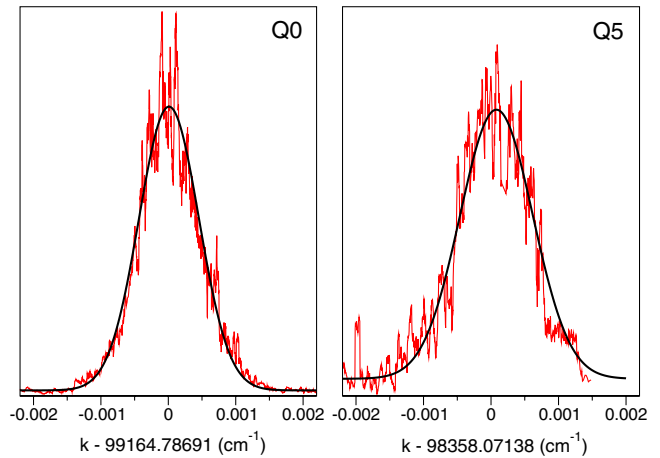

FIG. 2 (color online).   Recorded spectra of the Q0 and Q5 lines in the $EF - X$ (0,0) band using the methods discussed in the text.

are interconnected via 10 or more spectral transitions, a consistent framework of level energies with high accuracy can be constructed from the entire spectrum. For example, the rotational level energies in $B^1\Sigma_u^+$, $v = 2$ were determined from the analysis involving 13 different bands in the $EF - B$ system. The relative positioning of rovibrational level energies in the B state are determined from the analysis of several bands $EF - B$ and $GK^1\Sigma_g^+ - B$, while those of the C state result from the analysis involving the $I^1\Pi_g - C$, $J^1\Delta_g - C$, $H^1\Sigma_g^+ - C$ and $GK^1\Sigma_g^+ - C$ systems. The potential energy curves of the relevant excited states are depicted in Fig. 1(a). The bands connecting the C state are generally weaker than the bands belonging to the $EF - B$ system, and consequently, the reduced signal-to-noise ratio (SNR) leads to a greater uncertainty in the corresponding Werner lines.

Although all lines are Doppler broadened ($\Delta\nu_D = 0.02$–0.2 cm^{-1}, depending on the wavelength), the high
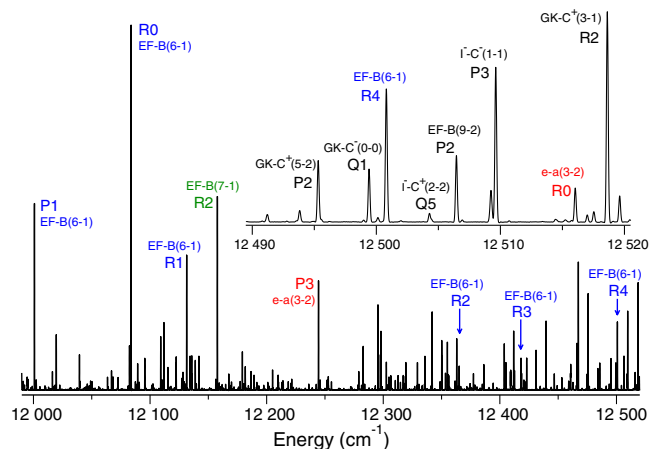

FIG. 3 (color online).   Sample spectrum obtained from the high-resolution Fourier-transform spectroscopy. The inset shows a smaller portion in detail.

SNR and the large amount of spectral information enables a statistical analysis that results in absolute accuracies of 10^{-4} cm^{-1} for the best lines, which are comparable to the uncertainty of the anchor lines ($<2 \times 10^{-4}$ cm^{-1}) [7]. The spectra were recorded multiple times at slightly varying conditions of pressure and discharge power. Each spectrum was calibrated against reference standard lines of CO [11] and Ar [12], for which purpose traces of CO and Ar were added in the discharge. Since the deduced level energies are obtained through transitions from many bands occurring at vastly different wavelengths in the FT-spectra, the absolute calibrations depend on a wide range of CO and Ar reference lines. For this reason, the uncertainty in the wavelength calibration is considered to be included in the statistical averaging process performed over the data ensemble. This comprehensive analysis leads to a highly accurate set of level energies of excited states that may be referenced to the $EF^1\Sigma_g^+$, $v = 0$ quantum states, with $J = 0$ for parahydrogen and $J = 1$ for orthohydrogen. In Table I, the level energies of the rotationless quantum states of $B^1\Sigma_u^+$, v and $C^1\Pi_u$, v levels are listed. The FT analysis includes a great number of quantum states, with vibrational quantum numbers covering $v = 0$–12 for the Lyman band and $v = 0$–2 for the Werner band. Most of these vibrational bands cover the range $J = 0$–7, with up to $J = 10$ for some strong bands.

Since the energies of rotationally excited states in the $EF^1\Sigma_g^+$, $v = 0$ band can be determined independently using either the FT- or DUV two-photon data sets, this allows for an independent check on the accuracy and consistency of each data set separately. The subsequent analysis of the relative level energies obtained from FT spectroscopy requires the $X^1\Sigma_g^+$ ground state level energies which are derived from the accurate far-infrared studies of Jennings *et al.* [13]. Relative to the lowest rotational state $J = 0$, we adopt X-state rotational excitation energies of 118.486 84(10) cm^{-1} for $J = 1$;

354.373 54(21) cm^{-1} for $J = 2$; 705.519 06(19) cm^{-1} for $J = 3$; 1168.798 27(22) cm^{-1} for $J = 4$; and 1740.189 30(19) cm^{-1} for $J = 5$. Using these ground state energy splittings in combination with the $Q0$ and $Q1$ lines of $EF - X$ (0,0), the anchor levels are determined for the para- and ortho- series, respectively. Performing a similar procedure with $Q2$ through $Q5$, obtained directly from the DUV spectroscopy, an independent determination of the EF ($v = 0$, $J = 2$–5) rotational energy levels E_{DUV} is obtained. A comparison of E_{DUV} to energy levels derived from the FT combination differences (referenced to the EF anchor lines) E_{FT} is shown in Table II. The difference $\Delta = E_{FT} - E_{DUV}$ falls within the stated 1σ uncertainty in E_{DUV}, where there is a considerable contribution due to the uncertainties in the ground state level energies. This comparison provides a strong verification of the accuracy of the separate (DUV- and FT-) data sets. Most importantly, this demonstrates the validity of the calculated values from the combination-difference method presented here.

From the large set of level energies of $B^1\Sigma_u^+$, v, J and $C^1\Pi_u$, v, J, ($\pm$) quantum states with respect to the $X^1\Sigma_g^+$, $v = 0$, $J = 0$ ground level, transition frequencies or wavelengths in the $B - X$ Lyman and $C - X$ Werner bands can then be calculated from the intercombination differences, taking into account the uncertainties deriving from both experiments. The R- and P-transition wavelengths for the lowest ortho and para rotational states in the Lyman band are listed in Table III, and a comprehensive list of the derived transitions is supplied in [17].

For the Lyman lines an average relative uncertainty of $\Delta\lambda/\lambda = 4.6 \times 10^{-9}$ is obtained, while the average for the Werner lines is $\Delta\lambda/\lambda = 1.7 \times 10^{-8}$. The derived transition wavelengths, compared to those obtained from direct extreme ultraviolet XUV laser excitation [2,14–16], are listed in Table III. As these example transitions demonstrate, there is good agreement between the present set of transition values and previous values from direct XUV measurements. Some systematic shifts appear in the $L5$–$L8$ bands, which we attribute to chirp effects in the pulsed-dye amplifier and in the harmonic conversion pro-

TABLE I. Level energies ν_0 of the rotationless ($J = 0$) quantum states in $B^1\Sigma_u^+$ and ($J = 1$) $C^1\Pi_u$ as obtained from the comprehensive analysis of the FT-data. The number N in BN and CN refers to the vibrational level, while the (+) and (−) refer to the Λ-doubling in the C state. The reference energy level is that of the EF, $v = 0$, $J = 0$ state. All values in cm^{-1}.

Level	ν_0	Level	ν_0
B0	−8961.287 13 (09)	B10	2700.147 38 (65)
B1	−7642.962 87 (40)	B11	3692.239 44 (49)
B2	−6361.486 56 (10)	B12	4654.734 66 (46)
B3	−5114.776 98 (12)	C0$^+$	−12.729 64 (48)
B4	−3901.759 84 (28)	C0$^-$	−13.936 00 (25)
B5	−2721.760 01 (24)	C1$^+$	2292.7827 (38)
B6	−1574.255 68 (33)	C1$^-$	2291.556 06 (45)
B7	−458.779 70 (30)	C2$^+$	4463.8750 (13)
B8	625.132 63 (30)	C2$^-$	4463.0752 (10)
B9	1677.944 89 (16)		

TABLE II. Comparison of the ($J = 2$–5) rotational level energies of the $EF^1\Sigma_g^+ - X^1\Sigma_g^+$ system obtained from direct DUV two-photon spectroscopy E_{DUV}, and those obtained from the indirect determination E_{FT} using the combined results of FT spectroscopy and $Q0$- and $Q1$-derived anchor lines from DUV spectroscopy. The difference, $\Delta = E_{FT} - E_{DUV}$, is also tabulated. All energies are expressed in cm^{-1}.

J	E_{DUV}	E_{FT}	Δ
0	99 164.786 91 (16)	para anchor	
1	99 228.218 23 (19)	ortho anchor	
2	99 354.556 55 (24)	99 354.556 31 (13)	−0.000 24
3	99 542.766 23 (24)	99 542.765 97 (19)	−0.000 26
4	99 791.325 26 (25)	99 791.325 06 (15)	−0.000 20
5	100 098.260 68 (24)	100 098.260 83 (17)	0.000 16

TABLE III. Comparison of combination-difference derived transition wavelengths λ_{FT} and direct XUV determination λ_{XUV} [2,14–16] for the first transitions of the Lyman $v = 0$–10 bands, expressed in nm. The difference, $\Delta = \lambda_{XUV} - \lambda_{FT}$ is in 10^{-6} nm. A full list of the derived data set is provided in [17].

Line	λ_{FT}	λ_{XUV}	Δ
$L0\,R(0)$	110.812 731 72 (16)	110.812 733 (7)	1.3
$L0\,P(1)$	111.006 255 79 (28)	111.006 251 (6)	−4.8
$L1\,R(0)$	109.219 519 99 (31)	109.219 523 (8)	3.0
$L1\,P(1)$	109.405 195 65 (54)	109.405 198 (6)	2.4
$L2\,R(0)$	107.713 865 76 (17)	107.713 874 (5)	8.2
$L2\,P(1)$	107.892 540 43 (27)	107.892 547 (5)	6.6
$L3\,R(0)$	106.288 206 97 (21)	106.288 214 (5)	7.0
$L3\,P(1)$	106.460 532 74(27)	106.460 539 (5)	6.3
$L4\,R(0)$	104.936 738 53 (22)	104.936 744 (4)	5.5
$L4\,P(1)$	105.103 245 71 (39)	105.103 253 (4)	7.3
$L5\,R(0)$	103.654 567 53 (20)	103.654 581 (4)	13.5
$L5\,P(1)$	103.815 704 53 (34)	103.815 713 (4)	8.5
$L6\,R(0)$	102.437 374 37 (49)	102.437 386 (5)	11.6
$L6\,P(1)$	102.593 518 51 (41)	102.593 535 (6)	16.3
$L7\,R(0)$	101.281 294 56 (51)	101.281 303 (5)	8.4
$L7\,P(1)$	101.432 716 35 (44)	101.432 724 (5)	7.6
$L8\,R(0)$	100.182 374 21 (33)	100.182 387 (5)	12.8
$L8\,P(1)$	100.329 650 33 (37)	100.329 662 (5)	11.7
$L9\,R(0)$	99.137 884 96 (28)	99.137 891 (5)	6.0
$L9\,P(1)$	99.280 962 53 (26)	99.280 968 (5)	5.5
$L10\,R(0)$	98.143 871 05 (76)	98.143 871 (5)	0.1
$L10\,P(1)$	98.283 529 70 (66)	98.283 533 (5)	3.3

cess in the Xenon nonlinear medium [18]. The present dataset is more accurate than that from direct XUV studies [2,14–16] for two main reasons: (1) the residual first-order Doppler shift at short wavelengths are circumvented; and (2) the main systematic uncertainty of chirp-induced effects of ~ 0.003 cm^{-1} is avoided.

If we consider only the 56 transitions (48 Lyman- and 8 Werner-lines) used in the recent $\Delta\mu/\mu$ analysis [2], the new set of wavelengths represents a 21-fold improvement for the Lyman lines and a sevenfold improvement for the Werner lines. Where the previous set of data, obtained from direct XUV laser spectroscopy at an accuracy of $\Delta\lambda/\lambda \sim 5.4 \times 10^{-8}$ [2,14–16] contributed for some 11% to the error budget in the $\Delta\mu/\mu$ analysis, the uncertainty contribution of the presently derived data set is only 1.7%, where half of this value is due to the 9 transitions that are outside the range of the present data set, where the XUV results are still used. Performing an identical analysis using the updated laboratory data yield $\Delta\mu/\mu = (2.74 \pm 0.59) \times 10^{-5}$.

In conclusion, we make available a laboratory data set of Lyman and Werner absorption bands in H_2, with a close-to-exact accuracy for the purpose of comparisons with high-redshift astrophysical data, to extract a possible variation of the proton-to-electron mass ratio. The order-of-magnitude improvement in the laboratory metrology will reduce the uncertainty contribution of the laboratory data to less than 2%, and any improvement on the derivation of the $\Delta\mu/\mu$ will fully depend on astrophysical observations using current telescope technology. Now that a new generation of telescopes with 30–40 m dishes are in the design stage, the present data may add to the scientific rationale for equipping these systems with spectrometers of much higher resolution than the existing ones.

[1] M. T. Murphy, J. K. Webb, and V. V. Flambaum, Mon. Not. R. Astron. Soc. **345**, 609 (2003).

[2] E. Reinhold, R. Buning, U. Hollenstein, A. Ivanchik, P. Petitjean, and W. Ubachs, Phys. Rev. Lett. **96**, 151101 (2006).

[3] W. Ubachs, R. Buning, K. S. E. Eikema, and E. Reinhold, J. Mol. Spectrosc. **241**, 155 (2007).

[4] V. V. Meshkov, A. V. Stolyarov, A. Ivanchik, and D. A. Varshalovich, JETP Lett. **83**, 303 (2006).

[5] A. Ivanchik, P. Petitjean, D. Varshalovich, B. Aracil, R. Srianand, H. Chand, C. Ledoux, and P. Boisseé, Astron. Astrophys. **440**, 45 (2005).

[6] P. Noterdaeme, C. Ledoux, P. Petitjean, F. Le Petit, R. Srianand, and A. Smette, Astron. Astrophys. **474**, 393 (2007).

[7] S. Hannemann, E. J. Salumbides, S. Witte, R. T. Zinkstok, E.-J. van Duijn, K. S. E. Eikema, and W. Ubachs, Phys. Rev. A **74**, 062514 (2006).

[8] S. Hannemann, E.-J. van Duijn, and W. Ubachs, Rev. Sci. Instrum. **78**, 103102 (2007).

[9] S. Hannemann, E. J. Salumbides, and W. Ubachs, Opt. Lett. **32**, 1381 (2007).

[10] D. Bailly and M. Vervloet, Mol. Phys. **105**, 1559 (2007).

[11] A. G. Maki, J. S. Wells, and D. A. Jennings, J. Mol. Spectrosc. **144**, 224 (1990).

[12] G. Norlén, Phys. Scr. **8**, 249 (1973).

[13] D. E. Jennings, S. L. Bragg, and J. W. Brault, Astrophys. J. **282**, L85 (1984).

[14] W. Ubachs and E. Reinhold, Phys. Rev. Lett. **92**, 101302 (2004).

[15] J. Philip, J. P. Sprengers, T. Pielage, C. A. de Lange, W. Ubachs, and E. Reinhold, Can. J. Chem. **82**, 713 (2004).

[16] T. I. Ivanov, M. O. Vieitez, C. A. de Lange, and W. Ubachs, J. Phys. B **41**, 035702 (2008).

[17] See EPAPS Document No. E-PRLTAO-101-035849 for molecular hydrogen $B - X$ Lyman ($v = 0$–12) and $C - X$ Werner ($v = 0$–3) transitions derived from the combination of Fourier-transform and deep-UV spectroscopies. For more information on EPAPS, see http://www.aip.org/pubservs/epaps.html.

[18] K. S. E. Eikema, W. Ubachs, W. Vassen, and W. Hogervorst, Phys. Rev. A **55**, 1866 (1997).